# Searching for the $T_{bc}$ molecular candidate via lineshape analysis

严茂俊

西南大学

2025 年 10 月 20 日

# Outline

# Motivation: predictions on the $T_{bc}$ with $J^P = 0^+$

## Deep bound state

- 11 MeV below $\bar{B}^0 D^0$ threshold M. Karliner et al, PRL 119 (2017)
- 23 MeV below $\bar{B}^0 D^0$ threshold in QM T. F. Caramés et al,PRD99 (2019)
- $39 \binom{+4}{-6} \binom{+8}{-18}_{latt.}$ MeV below $\bar{B}^0 D^0$ threshold A. Radhakrishnan et al, PRD 110(2024)
- $136 - 178.4\,\mathrm{MeV}$ below $\bar{B}^0 D^0$ threshold C.R. Deng et al EPJA 56 (2020); Y. Tan et al, EPJ.Plus 135 (2020);

## Shallow bound state

- $B_2 = 0.42 - 31.35\,\mathrm{MeV}$ in OBE, Ning Li et al, PRD 88(2013);M. Z. Liu et al, PRD 110(2024)
- $B_2 = 0.75 - 2.01\,\mathrm{MeV}$ in HEFT, Luciano M. Abreu,NPB 985 (2022)
- $B_2 = 1.7 - 8.4\,\mathrm{MeV}$ in V-exchange, S. Sakai et al, PRD96(2017)
- 4 MeV below $\bar{B}^0 D^0$ threshold in QM, G. Yang et al, PRD101 (2020)
- A few MeV below $\bar{B}D$ threshold, C. Alexandrou et al, PRL132 (2024)
- $B_2 = 0.8 - 3.6\,\mathrm{MeV}$ in ChEFT, Zhe Liu et al,PRD112(2025)

# $\bar{B}D$ FSI in $pp$ collision

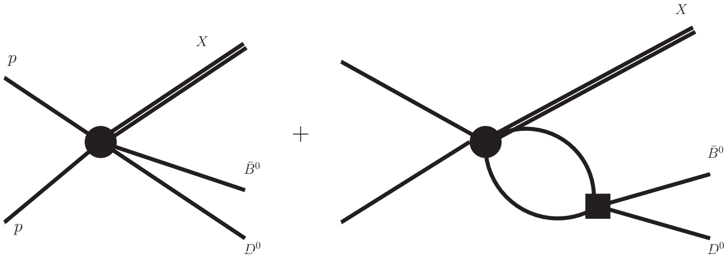


$th_2 - th_1 = 4.5\,\mathrm{MeV}$

- $|\bar{B}D\rangle_{I=0} = -\frac{1}{\sqrt{2}}|\bar{B}^0 D^0\rangle + \frac{1}{\sqrt{2}}|B^- D^+\rangle$,
  $|\bar{B}D\rangle_{I=1} = -\frac{1}{\sqrt{2}}|\bar{B}^0 D^0\rangle - \frac{1}{\sqrt{2}}|B^- D^+\rangle$
- $\bar{B}D$ FSI similar to the one of $ND$ in $\Lambda_b \to \pi^- p D^0$. S. Sakai et al,PLB808 (2020)
- Threshold effect in $\{\pi^0\pi^0, \pi^+\pi^-\}$ scattering, P. Budini et al,PRL6(1961);U.G. Meissner, PLB406(1997);J. Gasser et al, NPB 850 (2011); X.H. Liu et al, EPJC73(2013) ...

# ERE in $\bar{B}D$ FSI

## ERE in $\{\bar{B}^0 D^0,\ B^- D^+\}$ scattering

$$t_{ij} = \frac{2\pi}{\det}\begin{pmatrix} \frac{1}{\mu_1}\left(-\frac{1}{a_{22}}+ip_2\right) & -\frac{1}{a_{12}\sqrt{\mu_1\mu_2}} \\ -\frac{1}{a_{12}\sqrt{\mu_1\mu_2}} & \frac{1}{\mu_2}\left(-\frac{1}{a_{11}}+ip_1\right) \end{pmatrix}_{ij},$$

$$\det = \left(\frac{1}{a_{12}}\right)^2 - \left(\frac{1}{a_{11}}-ip_1\right)\left(\frac{1}{a_{22}}-ip_2\right),$$

$$\frac{1}{a_{22,\text{eff}}} = \frac{1}{a_{22}} - \frac{a_{11}}{a_{12}^2\left(1+a_{11}^2p_1^2\right)} - i\frac{a_{11}^2p_1}{a_{12}^2\left(1+a_{11}^2p_1^2\right)},$$

with $p_1 = \sqrt{2\mu_1(w-th_1)}$ and $p_2 = \sqrt{2\mu_2(w-th_2)}$.

- $\kappa = \sqrt{2\mu_2\delta} = O\left(\delta^{1/2}\right)$ with $\delta = m_{B^-} + M_{D^+} - m_{\bar{B}^0} - M_{D^0}$
- the isospin breaking difference $a_{22} - a_{11}$ is of $O(\delta)$ and neglected.

# Prodution amplitude

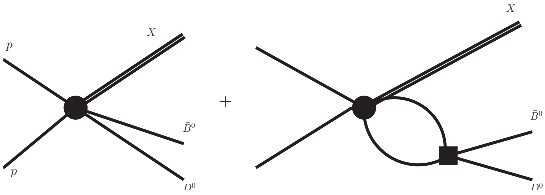


$$\mathcal{A} = V_P^\Lambda \left(1 + G^\Lambda_{\bar{B}^0 D^0} t_{\bar{B}^0 D^0, \bar{B}^0 D^0} + G^\Lambda_{B^- D^+} t_{B^- D^+, \bar{B}^0 D^0}\right)$$

- $V_P^\Lambda$ is scale (or cut-off) dependent and $G_i \propto \Lambda$
- $\mathcal{A}$ being cut-off independent leads to $V_P^\Lambda \propto 1/\Lambda$.

$$\mathcal{A} = V_P \left(t_{\bar{B}^0 D^0, \bar{B}^0 D^0} + t_{B^- D^+, \bar{B}^0 D^0}\right)$$

$$\frac{d\Gamma_{pp \to X \bar{B}^0 D^0}}{dM_{\bar{B}^0 D^0}} = \mathcal{N} p_X p_{D^0} \left| t_{\bar{B}^0 D^0, \bar{B}^0 D^0} + t_{B^- D^+, \bar{B}^0 D^0} \right|^2,$$

- $G^\Lambda_{\bar{B}^0 D^0} \simeq G^\Lambda_{B^- D^+}$; $\mathcal{N}$ is an overall normalization constant, $p_X$ $(p_{D^0})$ is the momentum of the $X$ $(D^0)$ in the $pp$ $(\bar{B}^0 D^0)$ rest frame

## $\{\bar{B}^0 D^0,\ B^+ D^-\}_B$ coupled scattering in ERE

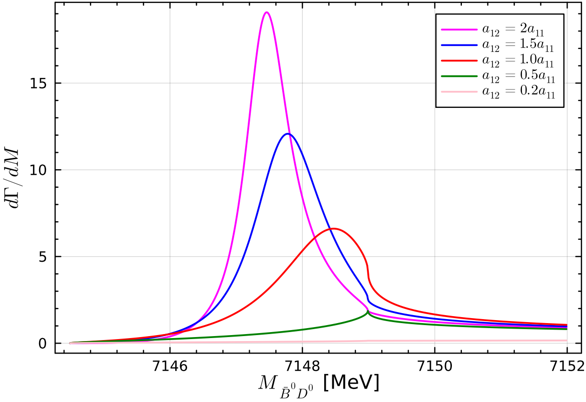


- the pink, green, red, blue, and magenta lines corresponding to $a_{22,eff} = 0.10 + i0.17\,\mathrm{fm}$, $0.18 + i1.42\,\mathrm{fm}$, $-2.66 + i1.77\,\mathrm{fm}$, $-2.91 + i0.69\,\mathrm{fm}$ and $-2.83 + i0.35\,\mathrm{fm}$ respectively.

# $\{\bar{B}^0 D^0,\ B^+ D^-\}_B$ coupled scattering in ERE

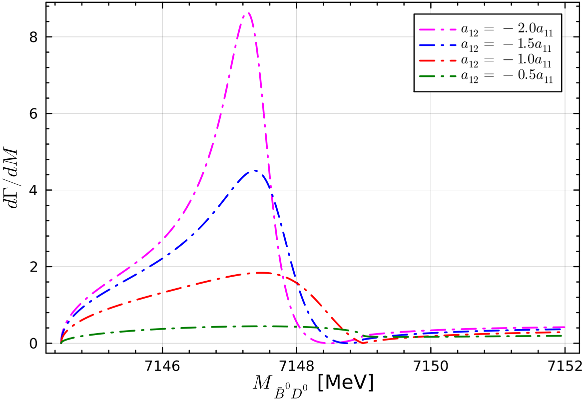


- the green, red, blue, and magenta lines corresponding to $a_{22,eff} = -0.18 + i1.42\,\mathrm{fm}, -2.66 + i1.77\,\mathrm{fm},\ -2.91 + i0.69\,\mathrm{fm},$ $-2.83 + i0.35\,\mathrm{fm}$ respectively.

# $\{\bar{B}^0 D^0,\ B^+ D^-\}_B$ coupled scattering in ERE

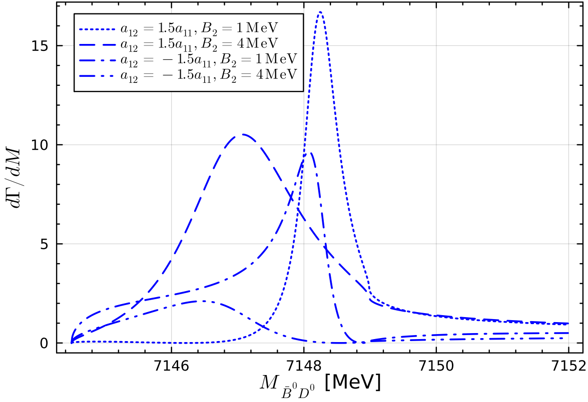


- the binding energy varies from 1 to 4 $\mathrm{MeV}$, where $a_{22,eff}$ is a function of $a_{12}^2$ and subsquently evaluated as $-3.95 + i0.74\,\mathrm{fm}$ and $-2.20 + i0.62\,\mathrm{fm}$ corresponding to the binding energies of 1 and $4\,\mathrm{MeV}$, respectively

# The feed-down effect from $D^*$ near $\bar{B}^0 D^0$ threshold

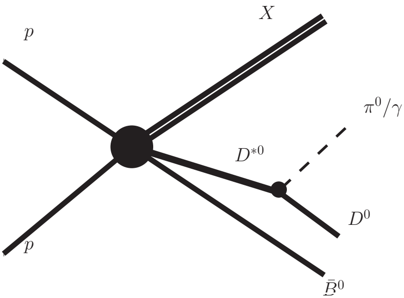


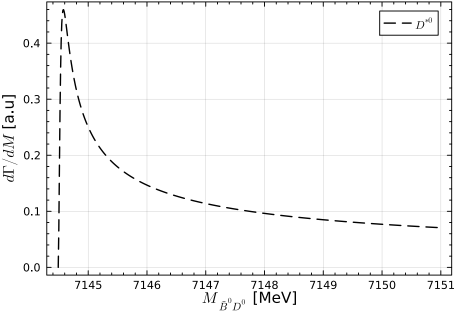


- The feed-down effect from $D^*$ causes a narrow enhancement near $\bar{B}^0 D^0$ threshold.
- The feed-down effect pollutes the enhancement from the pole in $\bar{B}D$ scattering.

# $\{\bar{B}^0 D^0,\ B^+ D^-\}_V$ coupled scattering in ERE

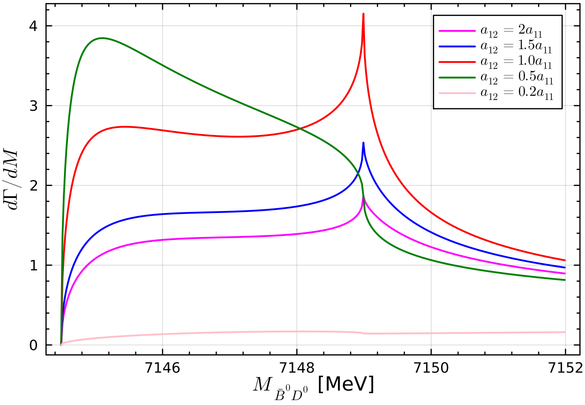


- $a_{22,eff}$ are $-0.10 + i0.17\,\mathrm{fm}$, $-0.18 + i1.42\,\mathrm{fm}$, $2.66 + i1.77\,\mathrm{fm}$, $2.91 + i0.69\,\mathrm{fm}$ and $2.83 + i0.35\,\mathrm{fm}$.
- Green: $-1/a_{22} + ip_2 - 1/a_{12} \simeq 2(-1/a_{22} - \kappa)$ @ $th_2$

# $\{\bar{B}^0 D^0,\ B^+ D^-\}_V$ coupled scattering in ERE

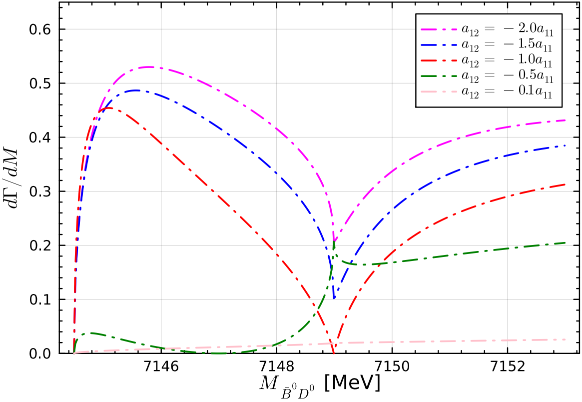


- $a_{22,eff}$ are $-0.03 + i0.04\,\mathrm{fm}$, $-0.18 + i1.42\,\mathrm{fm}$, $2.66 + i1.77\,\mathrm{fm}$, $2.91 + i0.69\,\mathrm{fm}$, and $2.83 + i0.35\,\mathrm{fm}$.
- Green: $-1/a_{22} + ip_2 - 1/a_{12} \simeq \mathcal{O}(1/a_{12})$ @ $th_2$

# $\{\bar{B}^0 D^0,\, B^+ D^-\}_V$ coupled scattering in ERE

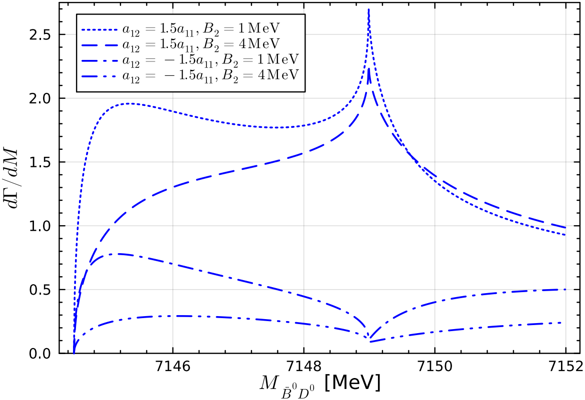


- $a_{22,eff}$ are $3.95 + i0.74\,\mathrm{fm}$ and $2.20 + i0.62\,\mathrm{fm}$.

# $\{\bar{B}_s^0 D^0,\ B^- D_s^+\}_B$ coupled scattering in ERE

$$|B^- D_s^+\rangle = \frac{1}{\sqrt{2}}|\bar{3}\rangle + \frac{1}{\sqrt{2}}|6\rangle,\ |B_s^0 D^0\rangle = -\frac{1}{\sqrt{2}}|\bar{3}\rangle + \frac{1}{\sqrt{2}}|6\rangle$$

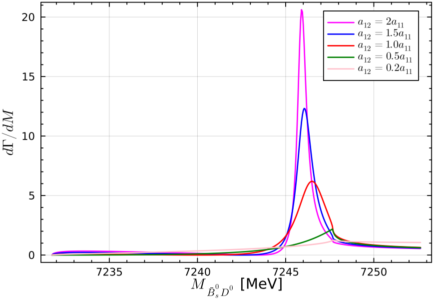


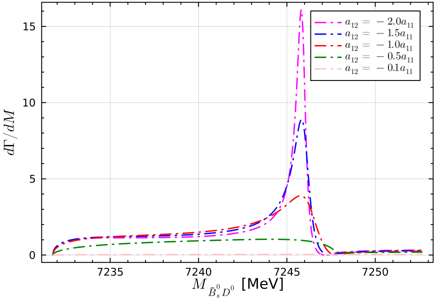


- $a_{22,eff} = 0.07 + i0.32\,\mathrm{fm},\ -0.78 + i1.76\,\mathrm{fm},\ -2.65 + i0.94\,\mathrm{fm},$ $-2.73 + i0.40\,\mathrm{fm}$ and $-2.71 + i0.22\,\mathrm{fm}$, respectively

# $\{\bar{B}_s^0 D^0,\ B^- D_s^+\}_V$ coupled scattering in ERE

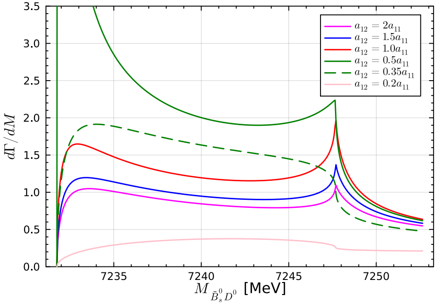


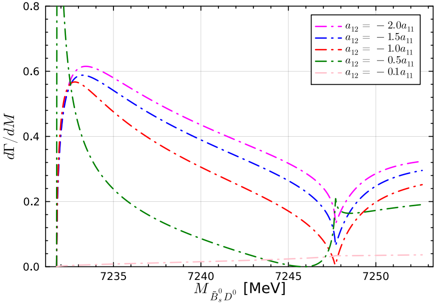


- $a_{22,eff} = 0.07 + i0.32\,\mathrm{fm},\ -0.78 + i1.76\,\mathrm{fm},\ -2.65 + i0.94\,\mathrm{fm},$ $-2.73 + i0.40\,\mathrm{fm}$ and $-2.71 + i0.22\,\mathrm{fm},$ respectively

# $\{\bar{B}_s^0 D^0,\ B^- D_s^+\}_V$ coupled scattering in ERE

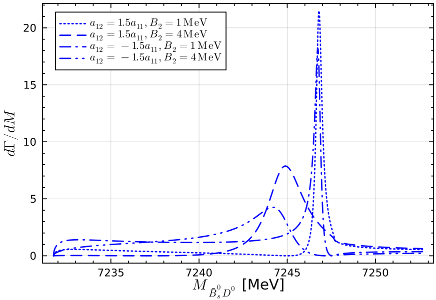


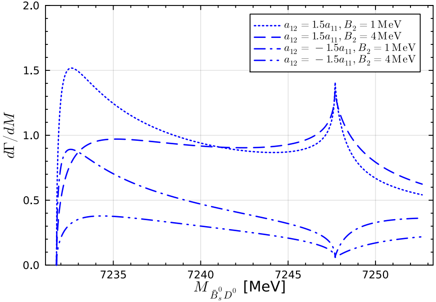


- $a_{22,eff} = -3.81 + i0.41\,\mathrm{fm}$, and $-1.98 + i0.39$ (left);
  $a_{22,eff} = 3.81 + i0.41\,\mathrm{fm}$ and $1.98 + i0.39\,\mathrm{fm}$ (right)
- a near threshold enhancement in $\bar{B}^0 D_s^+$ invaiant mass distribution in $\Upsilon \to D^- \bar{B}^0 D_s^+$ W.Y Liu et al; 2508.19007

# Summary

- $\{\bar{B}^0 D^0\,, B^- D^+\}$ coupled channel scattering is considered to search for the scalar $T_{bc}$ via the lineshape in $\bar{B}^0 D^0$ invariant mass distribution in pp collision.
- In the isospin limit with $a_{11} = a_{22}$, the interference between $t_{11}$ and $t_{21}$ plays a crucial role in generating the lineshapes.
- A new lineshape, differing from peak and cusp
- The feed-down effect from $D^*$ leads to a narrow enhancement around $th_1$.

- Extending to $\{pK^0,\, nK^+\}$ and $\{pD^0,\, nD^+\}$ scattering.
- $\{\Xi_c^+ K^-, \Xi_c^0 \bar{K}^0\}$ $\{D^0\Xi^0,\, D^+\Xi^-\}$ adopted to understand the $\Omega_c^*$.
- To understand the shoulder around $4.26\,\mathrm{GeV}$ in $e^+e^- \to J/\psi\pi^+\pi^-$.

# Summary

- $\{\bar{B}^0 D^0\,, B^- D^+\}$ coupled channel scattering is considered to search for the scalar $T_{bc}$ via the lineshape in $\bar{B}^0 D^0$ invariant mass distribution in pp collision.
- In the isospin limit with $a_{11} = a_{22}$, the interference between $t_{11}$ and $t_{21}$ plays a crucial role in generating the lineshapes.
- A new lineshape, differing from peak and cusp
- The feed-down effect from $D^*$ leads to a narrow enhancement around $th_1$.

- Extending to $\{pK^0,\ nK^+\}$ and $\{pD^0,\ nD^+\}$ scattering.
- $\{\Xi_c^+ K^-, \Xi_c^0 \bar{K}^0\}$ $\{D^0\Xi^0,\ D^+\Xi^-\}$ adopted to understand the $\Omega_c^*$.
- To understand the shoulder around $4.26\,\mathrm{GeV}$ in $e^+e^- \to J/\psi\pi^+\pi^-$.

***Thanks !***

# Backup

$$
\begin{aligned}
|\bar{B}D\rangle_{I=0} &= -\frac{1}{\sqrt{2}}|\bar{B}^0 D^0\rangle + \frac{1}{\sqrt{2}}|B^- D^+\rangle, \\
|\bar{B}D\rangle_{I=1} &= -\frac{1}{\sqrt{2}}|\bar{B}^0 D^0\rangle - \frac{1}{\sqrt{2}}|B^- D^+\rangle,
\end{aligned}
$$

$|\bar{B}^0 D^0\rangle = \frac{1}{\sqrt{2}}|6\rangle + \frac{1}{\sqrt{2}}|\bar{3}\rangle$ and $|B^- D^+\rangle = \frac{1}{\sqrt{2}}|6\rangle - \frac{1}{\sqrt{2}}|\bar{3}\rangle$.

$$
\begin{aligned}
V_{11} &= \langle \bar{B}^0 D^0|\mathcal{H}|\bar{B}^0 D^0\rangle = \frac{1}{2}V_6^{I=1} + \frac{1}{2}V_{\bar{3}}^{I=0}, \\
V_{12} &= \langle \bar{B}^0 D^0|\mathcal{H}|B^- D^+\rangle = \frac{1}{2}V_6^{I=1} - \frac{1}{2}V_{\bar{3}}^{I=0}, \\
V_{22} &= \langle B^- D^+|\mathcal{H}|B^- D^+\rangle = \frac{1}{2}V_6^{I=1} + \frac{1}{2}V_{\bar{3}}^{I=0},
\end{aligned}
$$

$$
G_i^\Lambda = \int^\Lambda \frac{d^3\mathbf{q}}{(2\pi)^3}\frac{2\mu_i}{\mathbf{q}^2 - p_i^2 - i\epsilon} = i\frac{\mu_i}{2\pi}p_i + \frac{\mu_i}{\pi^2}\Lambda\left[1 + O\left(\frac{p_i^2}{\Lambda^2}\right)\right].
$$

# Backup

$$
\begin{aligned}
t_{11}^{\mathrm{th}} &= \frac{2\pi}{\mu_1}\left(-\frac{1}{a_{22}}-\kappa\right)\left[\frac{1}{a_{12}^2}-\frac{1}{a_{11}}\left(\frac{1}{a_{22}}+\kappa\right)\right]^{-1} \\
&\simeq \frac{2\pi}{\mu_1}\left[\frac{1}{a_{22}}-\frac{1}{a_{12}^2\left(a_{11}^{-1}+\kappa\right)}\right]^{-1}, \\
t_{12}^{\mathrm{th}} &= -\frac{2\pi}{\sqrt{\mu_1\mu_2}}\frac{1}{a_{12}}\left[\frac{1}{a_{12}^2}-\frac{1}{a_{11}}\left(\frac{1}{a_{22}}+\kappa\right)\right]^{-1} \\
&\simeq -\frac{2\pi}{\sqrt{\mu_1\mu_2}}\frac{a_{11}}{a_{12}}\left(\frac{a_{11}}{a_{12}^2}-\frac{1}{a_{11}}-\kappa\right)^{-1},
\end{aligned}
$$

where $\kappa=\sqrt{2\mu_2\delta}$ with $\delta = m_{B^-}+M_{D^+}-m_{\bar{B}^0}-M_{D^0}$. One sees that $\kappa = O\left(\delta^{1/2}\right)$.

# Backup

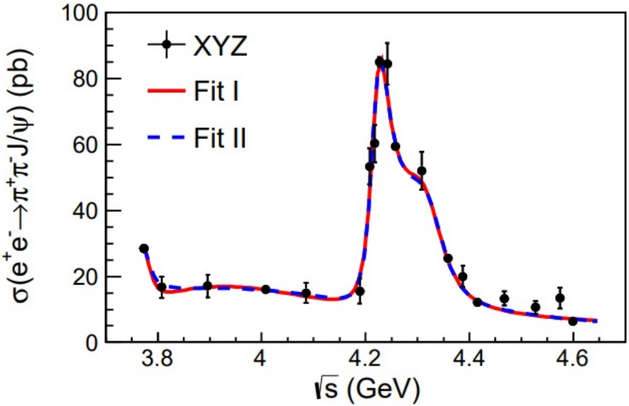

XYZ
Fit I
Fit II
$\sigma(e^+e^-\to\pi^+\pi^- J/\psi)$ (pb)
$\sqrt{s}$ (GeV)
0
20
40
60
80
100
3.8
4
4.2
4.4
4.6